Original paper

Novel metamaterials with negative moduli under compressive, tensile, and shear loadings

Sepehr Soltani, Reza Hedayati*

Department of Mechanical Engineering, K.N. Toosi University of Technology, Tehran, Iran

*Corresponding author. Email: rezahedayati@kntu.ac.ir

Abstract

Although mechanical metamaterials are rationally designed structures with micro-architectures that, in theory, can lead to any desirable mechanical properties, great interest has especially raised towards those with negative mechanical properties. In this paper, we propose structures that can show negative stiffness under shear, tensile, and hydrostatic loads. The principal working mechanism of the proposed structures is embedded pre-buckled and pre-twisted elements that can behave bistably. The structures demonstrated negative stiffness in a wide range of displacements under tensile and compressive loading types. Among the three model types, i.e. constant thickness, variable thickness, and variable column cases, in two cases (constant thickness and variable column), the structure demonstrated negative stiffness in a consecutive range of displacements over a large range of displacement values. The structure with variable thickness, on the other hand, demonstrated negative stiffness only in one displacement domain, and the structure behaved normally (i.e. with positive stiffness) in other displacement values. One can adjust the design parameters of lattice structure in order to get the negative and positive stiffness values in the desirable displacement values.

Keywords: Metamaterials; bi-stable; negative modulus; stiffness; lattice; 3d printing

1. Introduction

Metamaterials are artificial materials engineered to provide properties which "may not be readily available in nature" [1, 2]. These materials usually gain their properties from structure rather than composition, using the inclusion of small inhomogeneities to enact effective macroscopic behavior [3-7] .There are three major classes of metamaterial: Electromagnetic Metamaterials, Acoustic Metamaterials and Mechanical Metamaterials [2, 8-14].

Although mechanical metamaterials are rationally designed structures with micro-architectures that, in theory, can lead to any desirable mechanical properties, great interest has especially raised towards those with negative mechanical properties. This is because metamaterials with negative properties are not only capable of offering behaviors that conventional materials cannot accomplish, but the ability of rationally designing their micro-structure can result in counter-intuitive behaviors that can open up opportunities for designing materials and structures with ground-breaking novelties that inspire inventions. Negative properties that mechanical metamaterials can possess include, but are not limited to negative Poisson's ratio (NPR), materials that are commonly known as auxetics [15-18], negative thermal expansion (NTE) , negative compressibility (NC) [19], negative hygroscopic expansion (NHE) [20], negative moisture expansion (NME), and negative swelling [21].

Elastic modulus (also known as stiffness) represents the slope of the initially straight portion of the stress-strain of a material [22]. Unlike normal materials in which increasing the applied displacement increases the reaction force, in materials with negative stiffness it is expected to observed the inverse behavior. In other words, in a structure with negative elastic modulus, unlike what ius expected, if the structure is pushed, it pulls.

A number of research works have proposed structures with negative elastic modulus under compression load [23, 24]. To the best of our knowledge, no structures with negative stiffness under tensile, shear, and hydrostatic loadings have been proposed.

In this paper, we propose structures that can show negative stiffness under shear, tensile, and hydrostatic loads. The principal working mechanism of the proposed structures is embedded pre-buckled and pre-twisted elements that can behave bistably. Bistable mechanical systems having two local minima of potential energy can rest in either of the two stable equilibrium states in the absence of external loadings. A snap-through action may occur under suitable stimuli or loading, during which such systems exhibit distinct properties from linear structures [25]. Bistable structures are extensively used in industrial devices, such as switches [26, 27] whose sizes can vary from the macro-world to the micro-world [28], constant-force mechanisms [29-31] taking full advantage of negative stiffness characteristics of bistable configurations, energy harvesting devices [32-36] transforming ambient kinetic energy into electric power, actuators [37, 38] , and positioners.

In this work several types of structures with negative stiffness are proposed and analyzed numerically and experimentally. As for the numerical analysis, finite element modelling (FEM) is implemented. The range of negative stiffness values for each type of metamaterial is evaluated and the most effective geometrical aspects of the noted designs are pointed out.

2. Materials and Methods

2.1. Designs

Three designs were used for each metamaterial type proposed for compressive and tensile loading regimes. In the first design type, the beam and vertical column thicknesses were constant (Figure 1a). In the second design type, while the vertical column thicknesses were kept constant ($t = 1.27$

mm), the beam thicknesses decreased gradually from the top side of the specimens to the bottom side (Figure 1b). In the third design type, the curved beam thicknesses were kept constant ($t = 1.27$ mm), while the vertical column thicknesses gradually decreased from the top side of the specimen to its bottom side (Figure 1b). One of the designs (Figure 1a top) was already implemented in previous works [24], and we considered it here as well for comparison purposes.

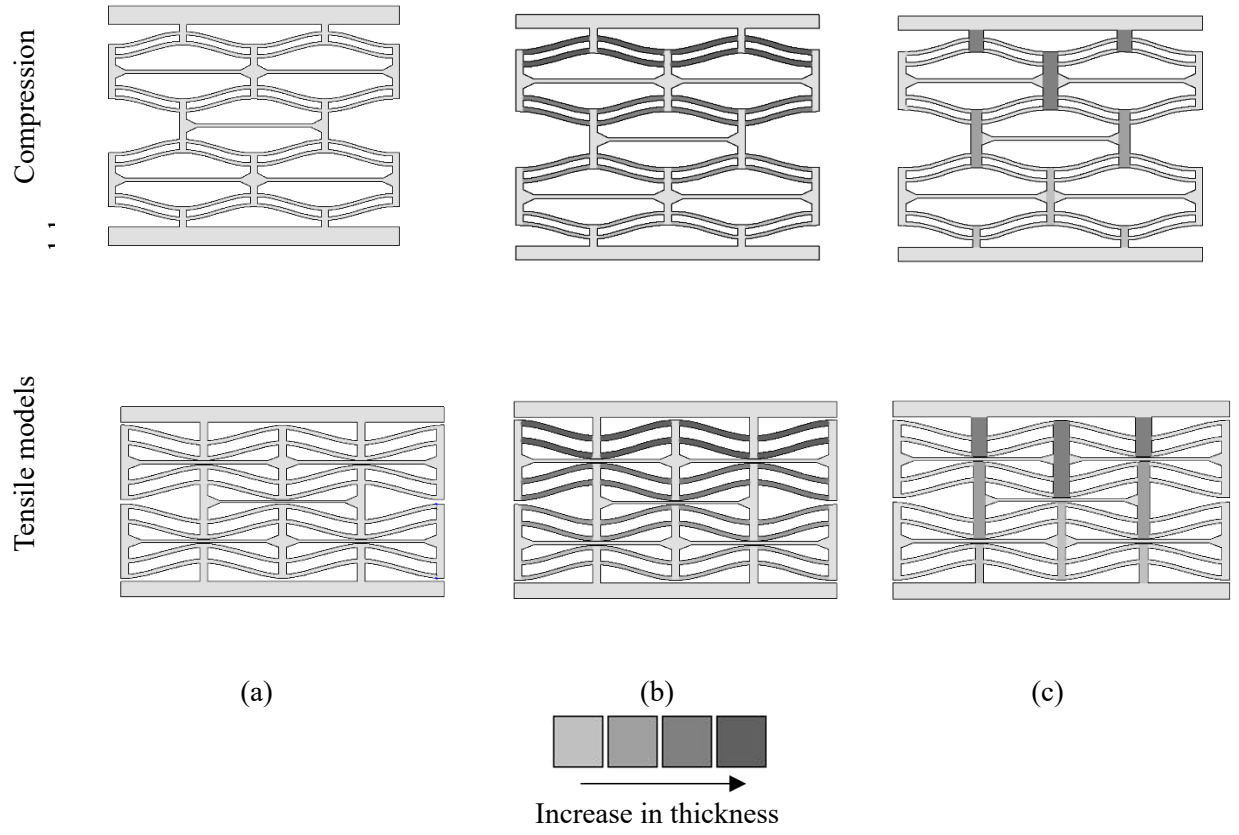

Figure 1: Different metamaterial design for accomplishing negative stiffness under compressive and tensile loadings: structures with (a) constant linkage thickness, (b) variable linkage thickness, and (c) variable column thickness.

For metamaterials with negative stiffness under shear loading, twist-based snap-through configurations were designed (see Figure 2). Two geometrical parameters, i.e. mid-plate thickness

and initial mid-plate twist, were varied respectively in the range of 1-8 mm and 10°-60°, and their effect on the apparent negative stiffness was observed.

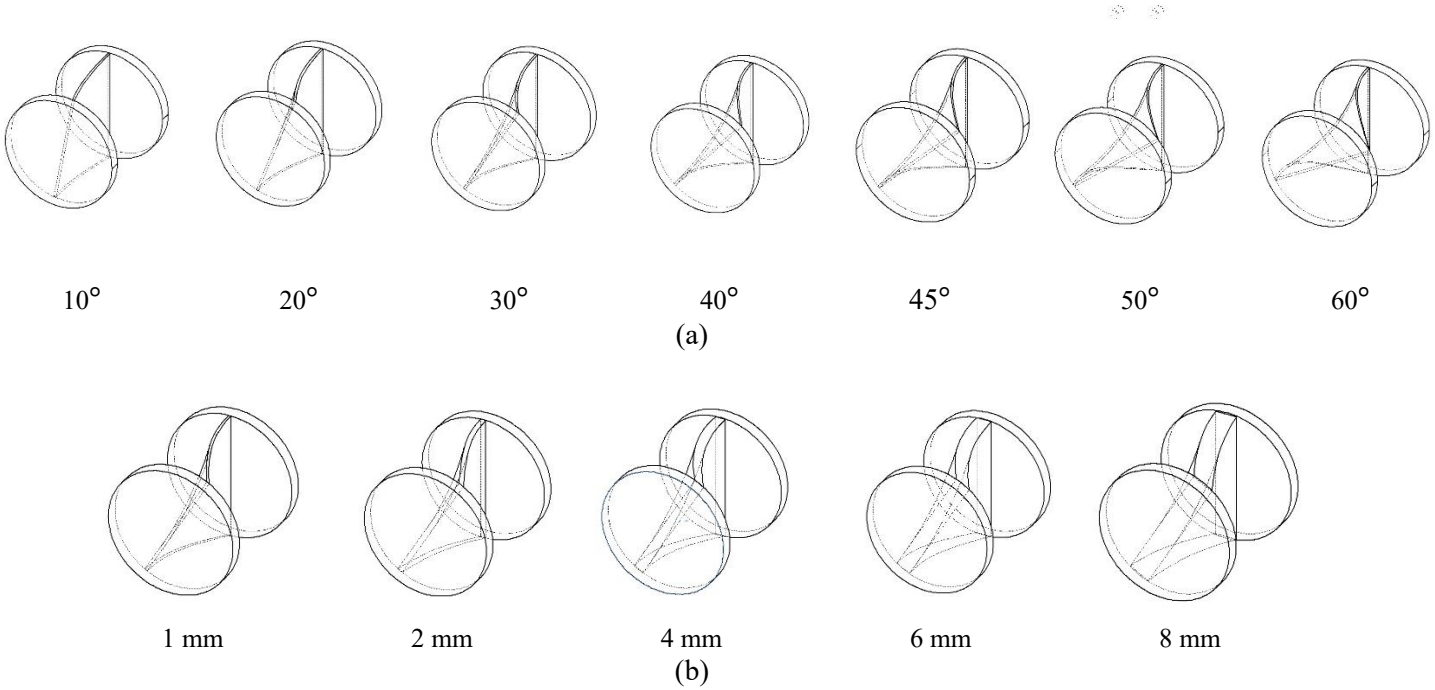

Figure 2: Different metamaterial designs for accomplishing negative stiffness under shear loading: structures having (a) different initial mid-plate twist angle, and (b) different mid-plate thickness.

2.2. Simulation

Numerical simulations were performed using commercial finite element package ABAQUS (Dassault Systèmes, France). The nonlinear problem was solved using implicit solver under quasi-static loading condition. Since the bistable snap-through behavior occurred in the elastic regime of the material, and no permanent plastic deformation was observed, only the elastic mechanical properties of nylon11 ($E = 1.58$ GPa and $\nu = 0.33$) were used as the input of the model. Frictionless tangential behavior was considered as the contact condition between the interacting surfaces. In tensile and compression analyses, the top faces of the models were uniformly displaced vertically, and a fixed boundary condition was applied at the bottom face of the structure. Similarly,

in the twist-based structures, the top plate was rotated, while the lower plate was kept fixed. Due to inability of tetrahedral and wedge to properly trace the local behavior of the material, linear hybrid hexahedral (C3D8H) elements were used for the analyses (see Figure S2 in the online Supplementary Material for the discretized structures).

3. Results

3.1. Negative stiffness under compression

The characteristic fluctuating force-displacement curves of structures with negative stiffness was observed in all the structure types (Figure 3). The force drop after each peak in the curve originated from snap through of rows of beams. This is a result of the change in the buckling mode of the curved beams from first buckling mode to third buckling mode (see Figure 4). In the case of the variable thickness structure (Figure 3b), the thinnest row demonstrated a snap-through behavior, and the next snap-throughs occurred sequentially in the beams in order of their thickness values. The structure with variable column thickness demonstrated more peaks and thorough compared to two other cases.

In the case of constant thickness structure, the second force peak value is very close to the first peak value (Figure 3a). The force values at the first peak and thorough were 228 N and 60 N respectively, showing a 73% decrease. However, in the case of the variable thickness structure, the second peak is greater (Figure 3b). Moreover, the variable thickness structure shows negative stiffness in a smaller range of displacements. Nonetheless, it is worth mentioning that in the noted small displacement region, the magnitude of negative stiffness in the structure with variable thickness beam is greater than that in the structure with constant thickness (-51 N/mm compared to -23 N/mm).

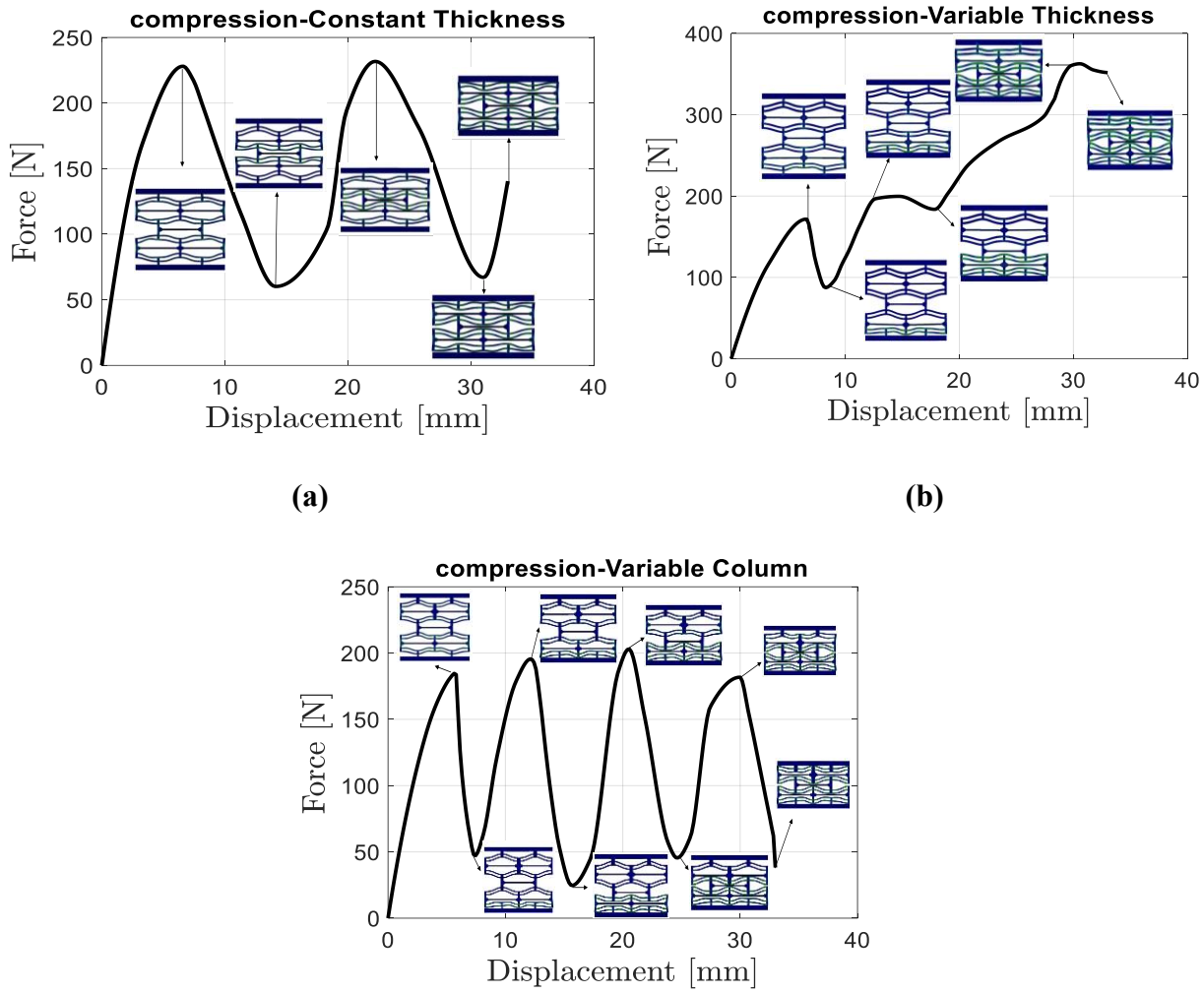

Figure 3: Force-displacement diagrams for compression models with (a) constant linkage thickness, (b) variable linkage thickness, and (c) variable column thickness.

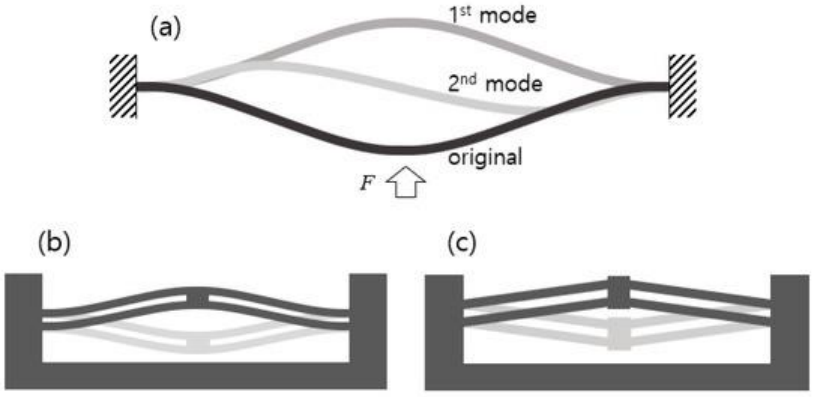

Figure 4: Shape sequence of buckling of beam

3.2. Negative stiffness under tension

Under tensile loading, the obtained force-displacement curves are very similar to those under compressive loading, although the force level values are lower. The other noted difference is that under tensile loading, for the case of constant thickness structures, the second peak of the force-displacement diagram does now show any significant change (i.e. it only shows 3 N increase, see Figure 3a), while under compressive loading, the second peak value is much higher than the first peak value (see Figure 5a).

The overall behavior of force-displacement curves of variable thickness and variable column structures is very similar under both tensile and compressive loading, although the force values and stiffness values in the case of compressive loading is greater than those under tensile loading (Figure 3b,c and Figure 5b,c).

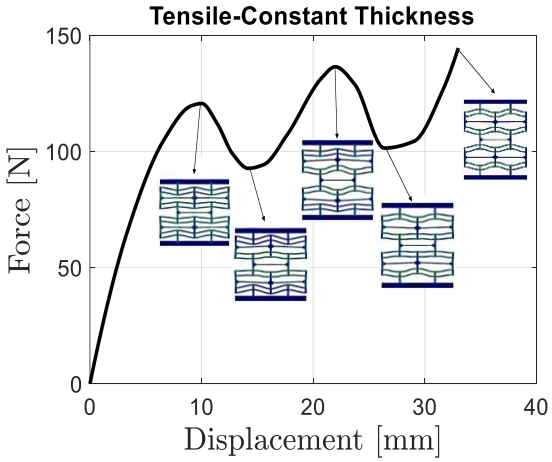

(a)

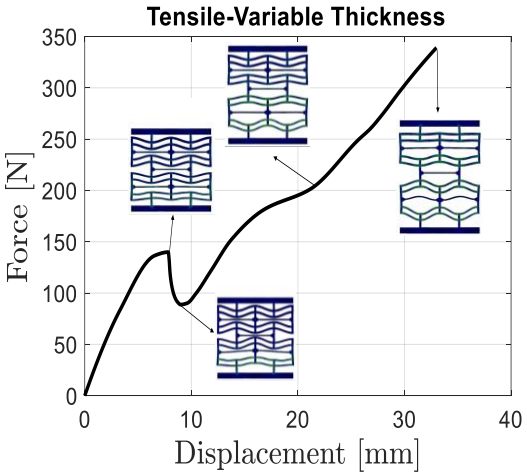

(b)

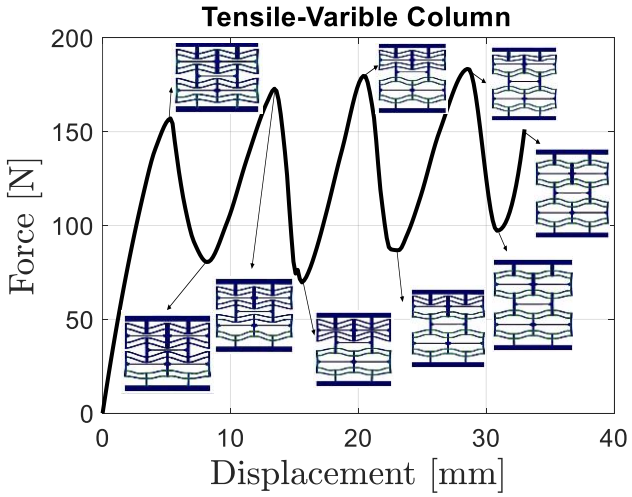

(c)

Figure 5: Force-displacement diagrams of different tensile models with: (a) constant linkage thickness, (b) variable linkage thickness, and (c) variable column thickness.

3.3. Negative stiffness under shear loading

Effect of mid-plate thickness (30 Degree)

In the first design, the effect of changing the thickness of the mid-plane was assessed. It can be seen that, as expected, by increasing the mid-plate thickness, the torque level values increase. Although the structures with lower mid-plate thicknesses demonstrated negative shear moduli, structures with mid-plate thicknesses greater than 6 mm consistently demonstrated positive stiffness values. Unlike the structures designed for tensile and compressive loadings, the twist-based designs showed only one peak in their diagrams and hence only one range of rotation in which negative stiffness could be observed. This can be explained by the fact that twist-based structures experience snap-through only once. The results of all curves are plotted in Figure 7 for comparison purposes.

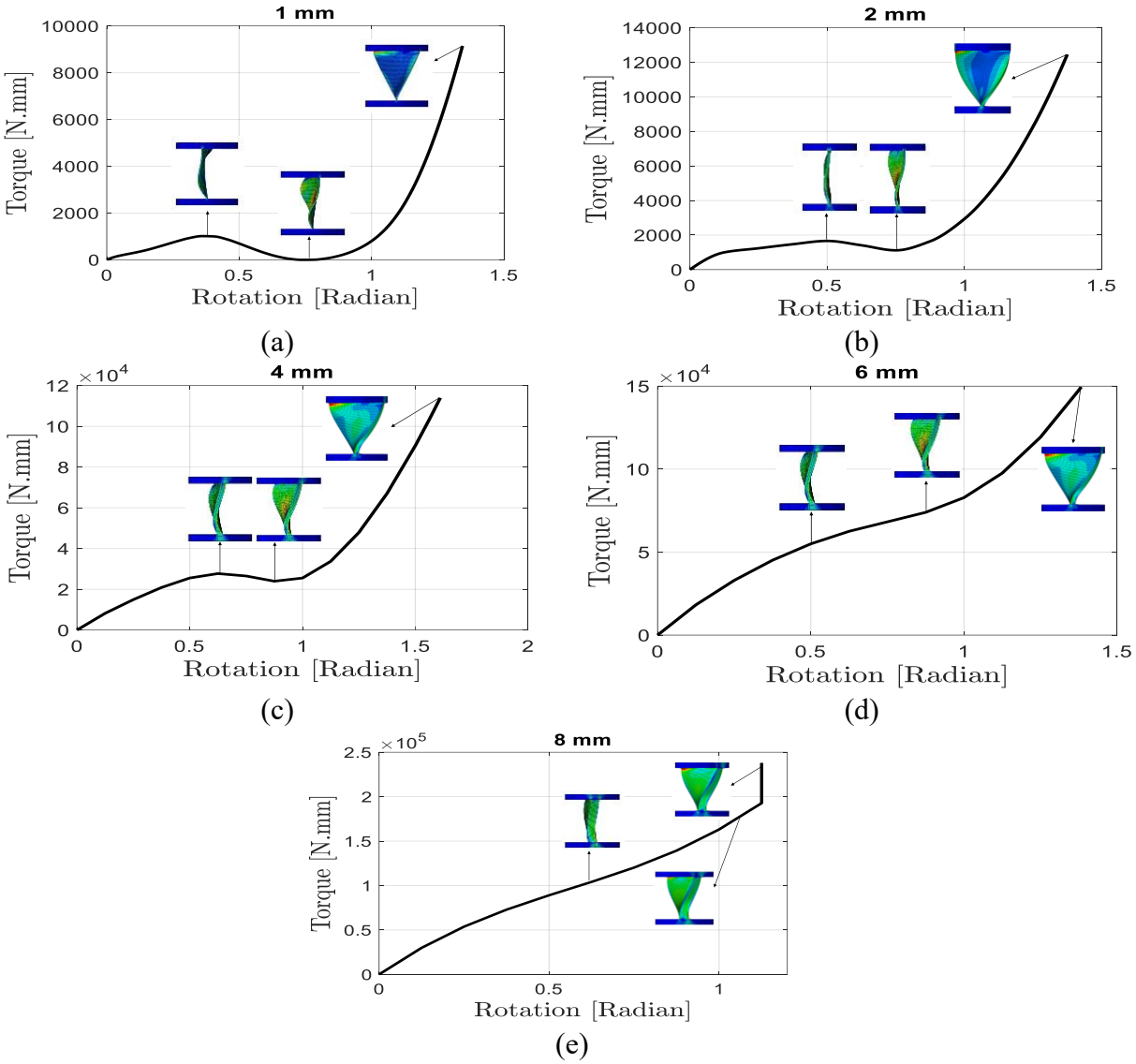

Figure 6: Torque-rotation curves of the torsion models with mid-plane thicknesses of (a) 1 mm, (b) 2 mm, (c)4 mm, (d) 6 mm, and (e) 8 mm.

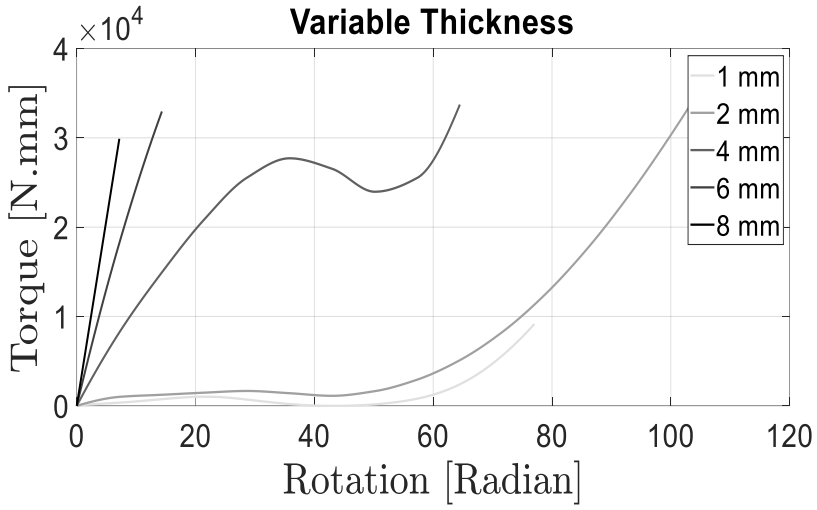

Figure 7: Comparison of torque-rotation curves of models with different mid-plate thicknesses

Effect of twist angle

The effect of mid-plane initial twist angle was evaluated for structures having mid-plate thickness of 1 mm. It can be seen that by increasing the thickness, the absolute value of the first peak as well as the absolute value of through increases (Figure 8 and Figure 9a). Increasing the initial twist angle also increases the range of possible rotation in the structure (Figure 9b). An interesting point is that the ratio of positive and negative stiffness values remains constant and around unity (Figure 9c). On the other hand, the ratio of peak to through values of torque is highly dependent on the mid-plane initial twist angle (Figure 9d).

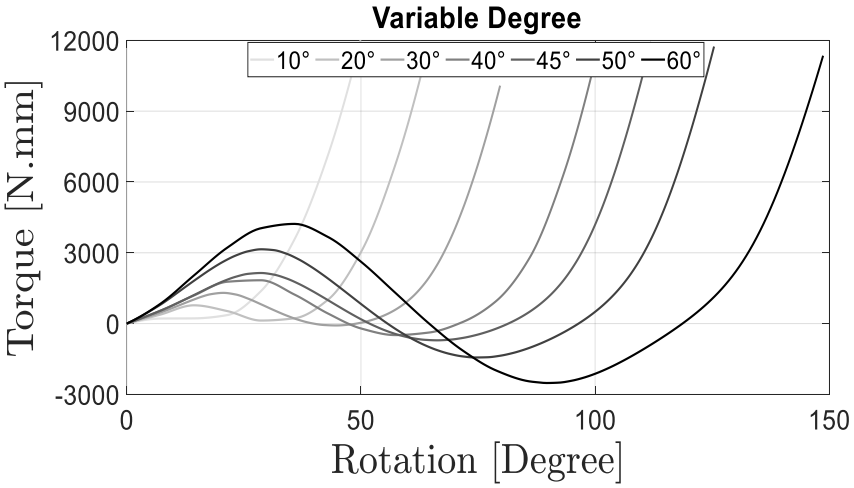

Figure 8: Comparison of torque-rotation curves of models with different initial mid-plate twists

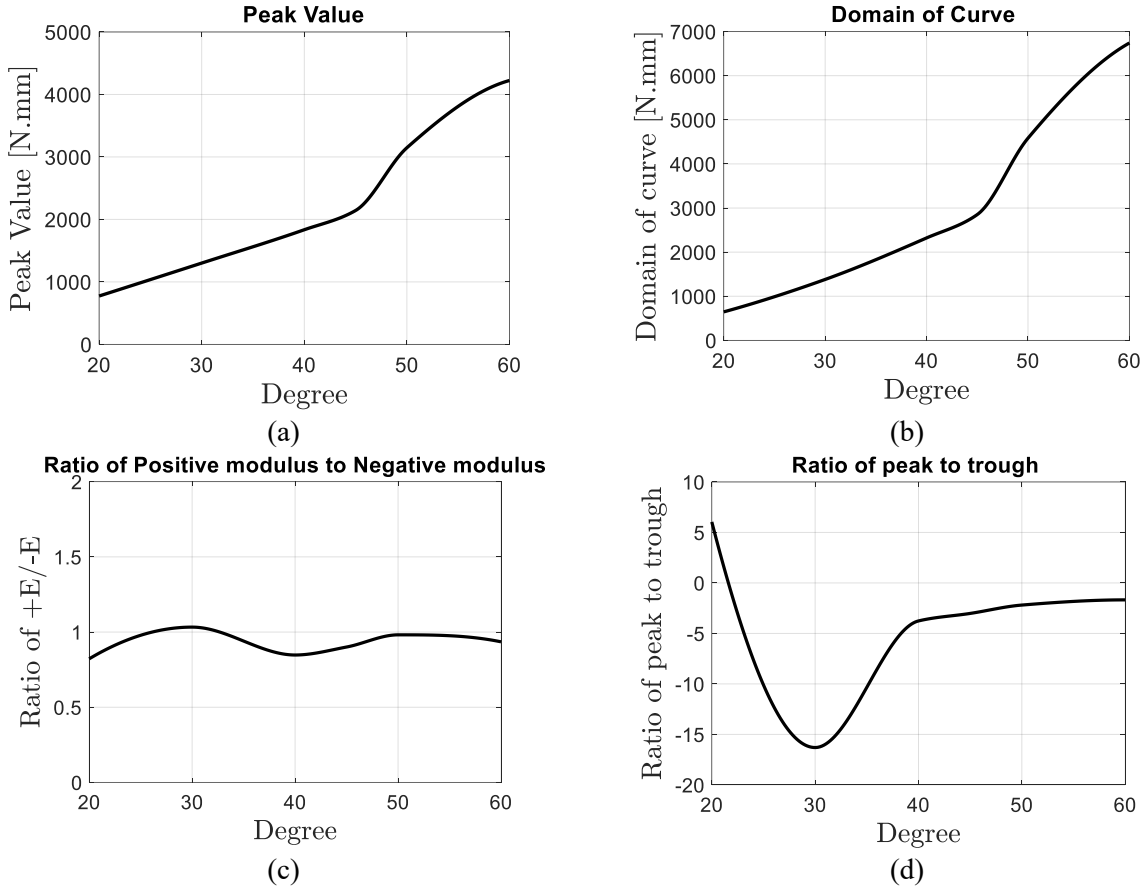

Figure 9: (a) Peak torque value, (b) range of torque, (c) ratio of positive modulus to negative modulus, and (d) ratio of peak to through values vs. mid-plane initial twist

4. Concluding remarks

In this work, we designed some metamaterial structures with negative stiffness under main mechanical loading types: tension, compression, and shear. The structures demonstrated negative stiffness in a wide range of displacements under tensile and compressive loading types. Among the three model types, i.e. constant thickness, variable thickness, and variable column cases, in two cases (constant thickness and variable column), the structure demonstrated negative stiffness in a consecutive range of displacements over a large range of displacement values. The structure with

variable thickness, on the other hand, demonstrated negative stiffness only in one displacement domain, and the structure behaved normally (i.e. with positive stiffness) in other displacement values. One can adjust the design parameters of lattice structure in order to get the negative and positive stiffness values in the desirable displacement values.

Reference

1. Ghavidelnia, N., S. Jedari Salami, and R. Hedayati, *Analytical relationships for yield stress of five mechanical meta-biomaterials.* Mechanics Based Design of Structures and Machines, 2020: p. 1-23.
2. Barchiesi, E., F. Di Cosmo, and M. Laudato, *A Review of Some Selected Examples of Mechanical and Acoustic Metamaterials*, in *Discrete and Continuum Models for Complex Metamaterials*, F.d.I.D.J. Steigmann, Editor. 2020, Cambridge University Press.
3. Mendhe, S.E. and Y.P. Kosta, *Metamaterial properties and applications.* International Journal of Information Technology and Knowledge Management, 2011. **4**(1): p. 85-89.
4. Roudbarian, N., et al., *Shape-memory polymer metamaterials based on triply periodic minimal surfaces.* European Journal of Mechanics-A/Solids, 2022. **96**: p. 104676.
5. Hedayati, R. and S. Lakshmanan, *Pneumatically-Actuated Acoustic Metamaterials Based on Helmholtz Resonators.* Materials, 2020. **13**(6): p. 1456.
6. Babaee, S., et al., *3D Soft metamaterials with negative Poisson's ratio.* Advanced Materials, 2013. **25**(36): p. 5044-5049.
7. Kolken, H.M. and A. Zadpoor, *Auxetic mechanical metamaterials.* RSC advances, 2017. **7**(9): p. 5111-5129.
8. Parveen, K., *Metamaterials: Types, applications, development, and future scope.* Intemational Journal of Advance Research, Ideas and Innovations in Technology, 2018. **4**(3): p. 2325-2327.
9. Hedayati, R., et al., *Improving the accuracy of analytical relationships for mechanical properties of permeable metamaterials.* Applied Sciences, 2021. **11**(3): p. 1332.
10. Chen, H. and C. Chan, *Acoustic cloaking in three dimensions using acoustic metamaterials.* Applied physics letters, 2007. **91**(18): p. 183518.
11. Hedayati, R. and M. Bodaghi, *Acoustic metamaterials and acoustic foams: recent advances.* Applied Sciences, 2022. **12**(6): p. 3096.
12. Schurig, D., et al., *Metamaterial electromagnetic cloak at microwave frequencies.* Science, 2006. **314**(5801): p. 977-980.
13. Hedayati, R. and S.P. Lakshmanan, *Active Acoustic Metamaterial Based on Helmholtz Resonators to Absorb Broadband Low-Frequency Noise.* Materials, 2024. **17**(4): p. 962.
14. Smith, F.C., F.L. Scarpa, and G. Burriesci. *Simultaneous optimization of the electromagnetic and mechanical properties of honeycomb materials*. in *Smart Structures and Materials 2002: Smart Structures and Integrated Systems*. 2002. SPIE.
15. Hedayati, R., et al., *Analytical relationships for 2D Re-entrant auxetic metamaterials: An application to 3D printing flexible implants.* journal of the mechanical behavior of biomedical materials, 2023. **143**: p. 105938.
16. Hedayati, R., M. Alavi, and M. Sadighi, *Effect of Degradation of Polylactic Acid (PLA) on Dynamic Mechanical Response of 3D Printed Lattice Structures.* Materials, 2024. **17**(15): p. 3674.

17. Chan, N. and K. Evans, *The mechanical properties of conventional and auxetic foams. Part I: compression and tension.* Journal of Cellular plastics, 1999. **35**(2): p. 130-165.
18. Hedayati, R., et al., *Gradient origami metamaterials for programming out-of-plane curvatures.* Advanced Engineering Materials, 2023. **25**(14): p. 2201838.
19. Nicolaou, Z.G. and A.E. Motter, *Mechanical metamaterials with negative compressibility transitions.* Nature materials, 2012. **11**(7): p. 608-613.
20. Lim, T.-C., *Negative hygrothermal expansion of reinforced double arrowhead microstructure.* physica status solidi (b), 2020. **257**(10): p. 1800055.
21. Lim, T.-C., *Mechanics of metamaterials with negative parameters*. 2020: Springer Nature.
22. Hibbeler, R.C., *Mechanics of Materials*. 2018: Pearson.
23. Qiu, J., J.H. Lang, and A.H. Slocum, *A curved-beam bistable mechanism.* Journal of microelectromechanical systems, 2004. **13**(2): p. 137-146.
24. Correa, D.M., et al., *Negative stiffness honeycombs for recoverable shock isolation.* Rapid Prototyping Journal, 2015. **21**(2): p. 193-200.
25. Cao, Y., et al., *Bistable structures for advanced functional systems.* Advanced Functional Materials, 2021. **31**(45): p. 2106231.
26. Kim, H., et al., *MEMS acceleration switch with bi-directionally tunable threshold.* Sensors and Actuators A: Physical, 2014. **208**: p. 120-129.
27. Andò, B., et al., *A bistable buckled beam based approach for vibrational energy harvesting.* Sensors and Actuators A: Physical, 2014. **211**: p. 153-161.
28. Zhou, Z., W. Qin, and P. Zhu, *Improve efficiency of harvesting random energy by snap-through in a quad-stable harvester.* Sensors and Actuators A: Physical, 2016. **243**: p. 151-158.
29. Huynh, B. and T. Tjahjowidodo, *Experimental chaotic quantification in bistable vortex induced vibration systems.* Mechanical Systems and Signal Processing, 2017. **85**: p. 1005-1019.
30. Song, G.-E., K.-H. Kim, and Y.-P. Lee, *Simulation and experiments for a phase-change actuator with bistable membrane.* Sensors and Actuators A: Physical, 2007. **136**(2): p. 665-672.
31. Gerson, Y., et al., *Design considerations of a large-displacement multistable micro actuator with serially connected bistable elements.* Finite Elements in Analysis and Design, 2012. **49**(1): p. 58-69.
32. Fotsa, R.T. and P. Woafo, *Chaos in a new bistable rotating electromechanical system.* Chaos, Solitons & Fractals, 2016. **93**: p. 48-57.
33. Saif, M.T.A. and N.C. MacDonald, *A millinewton microloading device.* Sensors and Actuators A: Physical, 1996. **52**(1-3): p. 65-75.
34. Plaut, R.H., *Snap-through of arches and buckled beams under unilateral displacement control.* International Journal of Solids and Structures, 2015. **63**: p. 109-113.
35. Samuel, B., A. Desai, and M. Haque, *Design and modeling of a MEMS pico-Newton loading/sensing device.* Sensors and Actuators A: Physical, 2006. **127**(1): p. 155-162.
36. Huang, Y., J. Zhao, and S. Liu, *Design optimization of segment-reinforced bistable mechanisms exhibiting adjustable snapping behavior.* Sensors and Actuators A: Physical, 2016. **252**: p. 7-15.
37. Zhang, Q., et al., *Design and fabrication of a laterally-driven inertial micro-switch with multi-directional constraint structures for lowering off-axis sensitivity.* Journal of Micromechanics and Microengineering, 2016. **26**(5): p. 055008.
38. Cazottes, P., et al., *Bistable buckled beam: modeling of actuating force and experimental validations.* 2009.